

Flexural Behavior of RC One-Way Slabs Strengthened with Fiber Reinforcement Cementations Matrix, FRCM.

Ali Hadi Adheem,

Kerbala Technical Insitute, Al-Furat Al-Awsat Technical University, 56001 Kerbala, Iraq.

ali.hadi@kit.edu.iq

Isam M. Ali

Karbala Technical Insitute, AL-Furat AL-Awsat Technical University, 56001 Kerbala, Iraq.

ali_isam@ymail.com

Mustafa S. Shaker

Karbala Technical Insitute, AL-Furat AL-Awsat Technical University, 56001 Kerbala, Iraq.

aldulaimy.mustafa93@gmail.com

Submission date:- 3/10/2018	Acceptance date:-21/10/2018	Publication date:- 18/11/2018
------------------------------------	------------------------------------	--------------------------------------

Abstract:

Numerical simulation performed in this paper to explore the flexural behavior of RC one way slab strengthened with fiber reinforcement cementations matrix (FRCM). Three dimensional finite element analysis was performed by using ANSYS (17.2). The main issues focused in this paper are (1) the effect of FRCM fabric types on the flexural behavior of strengthened RC slab in terms of both ultimate capacity and deflection, (2) effect of variables compressive strength value of the concrete slab and (3) number of fabric layers for composite material effect. The results showed that the fabric type had a clear effect on the flexural behavior of the strengthened slab. The parametric study also revealed that the flexural strength increases with increasing the compressive strength of concrete when the failure is represented by crushing of the concrete strut. In addition to, the number of fabric layers for composite material had a clear effect on the behavior of RC slab, but to a specified number because then the failure is determined by the action of the concrete in the compression zone.

Key words: Fiber reinforcement, One-way, FRCM composite, Strengthen.

1. Introduction

Structural elements have deteriorated in recent years due to environmental conditions or increased loads. Composite fiber (FRP) is one technique used to strengthen structural elements. This technique has been widely used in civil engineering society because of the materials properties, namely: corrosion resistance, ratio of extremely high strength-to-weight, ease and speed of application and minimal change in the geometry, [1]. In spite of all these advantages, the FRP strengthening technique has a little disadvantages, which are attributed to the resins used to bind or impregnate the fibers, [2]. These defects may include: (A) Poor bonding between the FRP and the concrete substrate. (B) Degradation of bonding material at high temperatures; (C) Epoxy is relatively expensive, (D) In the case of wet surfaces or low temperature FRP cannot be applied; (E) The concrete structure is gradually damaged by lack of vapor permeability, F) Semi-adhesive materials are not compatible with epoxy resins; (G) In the event of an earthquake, the condition of the concrete cannot be assessed behind FRP. Inorganic binders are one possible solution to the problems mentioned above, for example. Cement-based mortar, leading to the replacement of FRP with fiber reinforced mortar (FRMs), [3]. [4], used of glass, basalt, and carbon fiber girds for strengthening reinforced concrete one-way slabs. The strengthened slabs with carbon fiber grid exhibited a higher load carrying capacity and a higher displacement ductility performance before failure than the strengthened slabs with glass or basalt fibers. [5], studied the effect of the FRCM strengthening system on the flexural behavior of RC beams. Results explained the ultimate load increased from 10% to 44% when compared with un-strengthened beams. [6], studied the flexural behavior of RC beams strengthening by FRCM. Laboratory experiments showed that flexural resistance to the RC beams improved with FRCM technology.

Depending on the quantity of FRCM, flexural strength improved by 32% for one ply of the FRCM and 92% for four plies of the FRCM with low-strength concrete, and 13% for one ply of the FRCM and 73% for four plies of the FRCM with high-strength concrete. [7], improved behavior and performance of reinforced structural elements using polymeric fiber. The practical results showed good compatibility with the analytical models for maximum displacement and strength capacity. [8], demonstrated an experimental campaign for flexural strengthening of RC beams with carbon fiber polymers and steel fiber-reinforced polymers (SRP). [9], shows that the steel cords and carbon fibers give close results, when the steel ratio is similar. For low-density steel cords bonded with cementitious grout gave a low tension stiffening effect. The impact of SRG / SRP on the behavior of concrete slabs was studied by [10]. Laboratory testing shows that the performance of RC slabs improves with both the number of layers and the density of polymers. The percentage of increase in load capacity was ranging from 40% to 90% based on the type of steel wires (low/high density), the number of layers, and the type of adhesive (epoxy/grout).

The main objective of the current research is to expand the existing information base on numerical models of FRCM used in flexural strengthening of RC one-way slab. The FE models are developed for the experimental beams tested by [11]. The FE models present different non-linear models for the concrete (in tension and compression), steel reinforcement, CFRP laminate, cementitious matrix, different fabric material and the bond interface between the composite materials and concrete. The current study intends to provide a comprehensive understating of the effects of larger number of variables that may affect the contribution of this technique. These parameters are including such as concrete compressive strength, with various FRCM layers and different fabric types of composite materials. The composites materials that used in this study were polyparaphenylene benzobisoxazole (PBO) with a cementitious-based curing agent (FRCM), carbon fiber grid with polymer curing agent (CFRP-grid), and glass fiber grid (GLASS-grid).

2. Summary of experiments

This finite element analysis (FEA) calibration study includes modeling a concrete slab with the dimension and properties corresponding to solid slab tested by [11], with span equal to 1800 mm, tested under four-point bending. All specimens contain of flexural reinforcement [$3\phi 8$ mm] as tensile rebar. The test setup represented in Fig. 1 was used, and the two laminate arrangement, illustrated in Table (1), were adopted. The experimental study include: one RC slab without strengthening and two with differential of NSM-CFRP percentage (ρ_f). The average compressive strength (f_c) = 41.74 MPa. Table (2) includes the experimental tests values carried out to evaluate the main properties of the materials used in the present work.

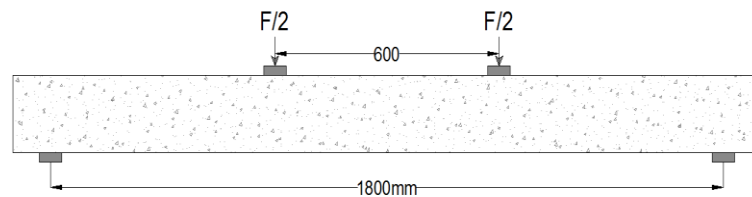


Fig. (1): Test setup configuration.

Table (1): Specimen's cross section details [11].

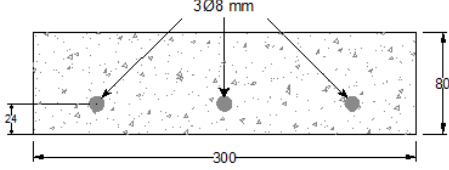
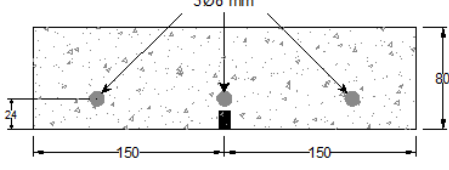
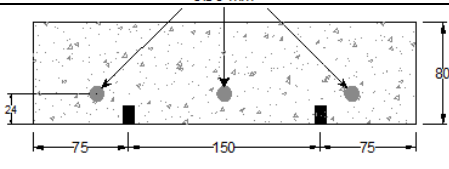
Slab symbol	Cross section (dimensions in mm)	No. of laminates	(ρ_f) %
S1		0	0
S2		1	0.06
S3		2	0.13

Table (2): Characteristics the steel reinforcement, laminates and epoxy adhesive [11].

Steel reinforcement	CFRP laminate	Laminate adhesive
$\phi_s = 8mm$ $E_s = 200.8GPa$ $f_y = 438.2 MPa$ $f_u = 578.75 MPa$	$t_f = 1.4 mm$ $w_f = 10.02 mm$ $E_f = 161 GPa$ $f_u = 1776.35 MPa$	$E_a = 7.47 GPa$ $f_u = 33.03 MPa$ $\epsilon = 4.83\%$

3. Finite element modeling

ANSYS software program (17.2) [12] utilized in this research for numerical simulation of the strengthened RC slab beneath four-point bending tests.

3.1. Elements description

- 1- Solid 65 was used to model both concrete slab and mortar for the FRCM. This element is suitable to model concrete due to its ability to crushing in compression and cracking in tension. Each node in SOLID65 has three translation degrees of freedom (x, y and z).
- 2- 3D 2-node structural bar element (LINK188) is using to model the flexural reinforcement. This element is capable of plastic deformation, which may occur in the steel reinforcement.
- 3- CFRP laminates, adhesives, and the steel plates that are placed between concrete and loading apparatus or supports were modelled using 8-node brick element (solid 185). The element also has eight nodes; each node has three degrees of freedom, translations in the global directions (x, y, and z), and is eligible to consider nonlinear properties like plasticity, multi-linear material model, stress stiffening, and large deformations. Last part of this model is the interaction among the composite materials and concrete beam which was modelled using a surface-to-surface contact pairs. This was undertaken by defining the adhesive as a contact surface using CONTA173. This element (CONTA173) is defined by four nodes. More information about the definition of these elements is identified later on.

These elements were used in the finite element model shown in Fig. (2).

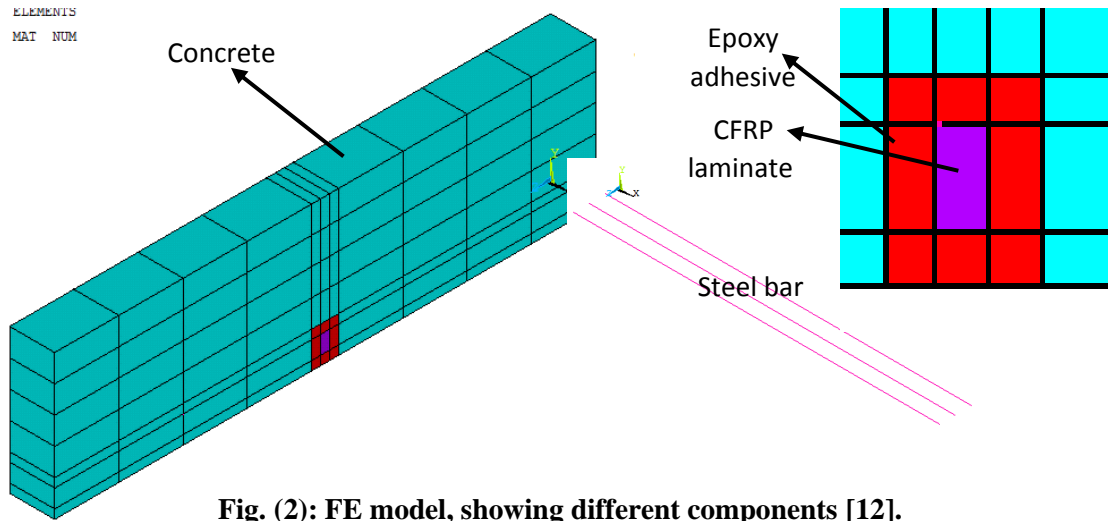


Fig. (2): FE model, showing different components [12].

3.2. Material modelling

3.2.1. Concrete

Fig. (3a), shown a nonlinear stress-strain model, suggest by [13], is utilized to simulate uniaxial compressive behavior of concrete. Mathematical expression to define concrete model is showed below.

$$f_c = f'_c \left[2 \left(\frac{\varepsilon}{\varepsilon_0} \right) - \left(\frac{\varepsilon}{\varepsilon_0} \right)^2 \right] \quad (1)$$

Where:

f_c is the compressive stress at any strain (ε);

ε_0 is the strain at f'_c , which can be calculated from equation (2)

$$\varepsilon_0 = \frac{2f'_c}{E_c} \quad (2)$$

E_c is the concrete elastic modulus which can be calculated following [14] as in equation (3)

$$E_c = 4700\sqrt{f'_c} \quad (3)$$

The concrete tensile stress-strain response is modeled as linear elastic prior to the onset of cracking at a maximum tensile stress which can be obtained as in equation (4)

$$f_t = 0.56\sqrt{f'_c} \quad (4)$$

Tension-stiffening effects are modelled with a linear descending curve ending at a strain of $6\varepsilon_t$, where ε_t is the strain at f_t (Fig. (3b)). A value of 0.3 was used for the open and closed shear transfer coefficients [15]. The Poison's ratio of concrete is assumed to be 0.2.

3.2.2. Steel reinforcement

The longitudinal rebars were assumed to have an elastic-perfectly plastic stress-strain response, identical in tension and compression, see Fig. (3c) poisson's ratio of 0.3 was assigned to the material, [16].

3.2.3. CFRP laminate

An isotropic linear elastic behavior is assigned for CFRP laminates, see Fig. (3c). A failure criteria is characterized for each component. The linear response is supposed to continue until the

tensile strength is reached, and beyond that a complete tensile failure is assumed. A Poisson's ratio of 0.3 was assigned for CFRP components and of 0.35 for adhesives, [17].

3.2.4. FRCM composite

To model the polyparaphenylene benzobisoxazole (PBO), carbon fiber grid (CFRP-grid) and glass fiber grid, material orthotropic-elastic material. This material is adequate for modeling the elastic-orthotropic behavior of solids, shells, and thick shells. The fundamental parameters required in this model are E, PR, and shear modulus G in three orthogonal directions, and fiber direction is characterized by a vector, [18].

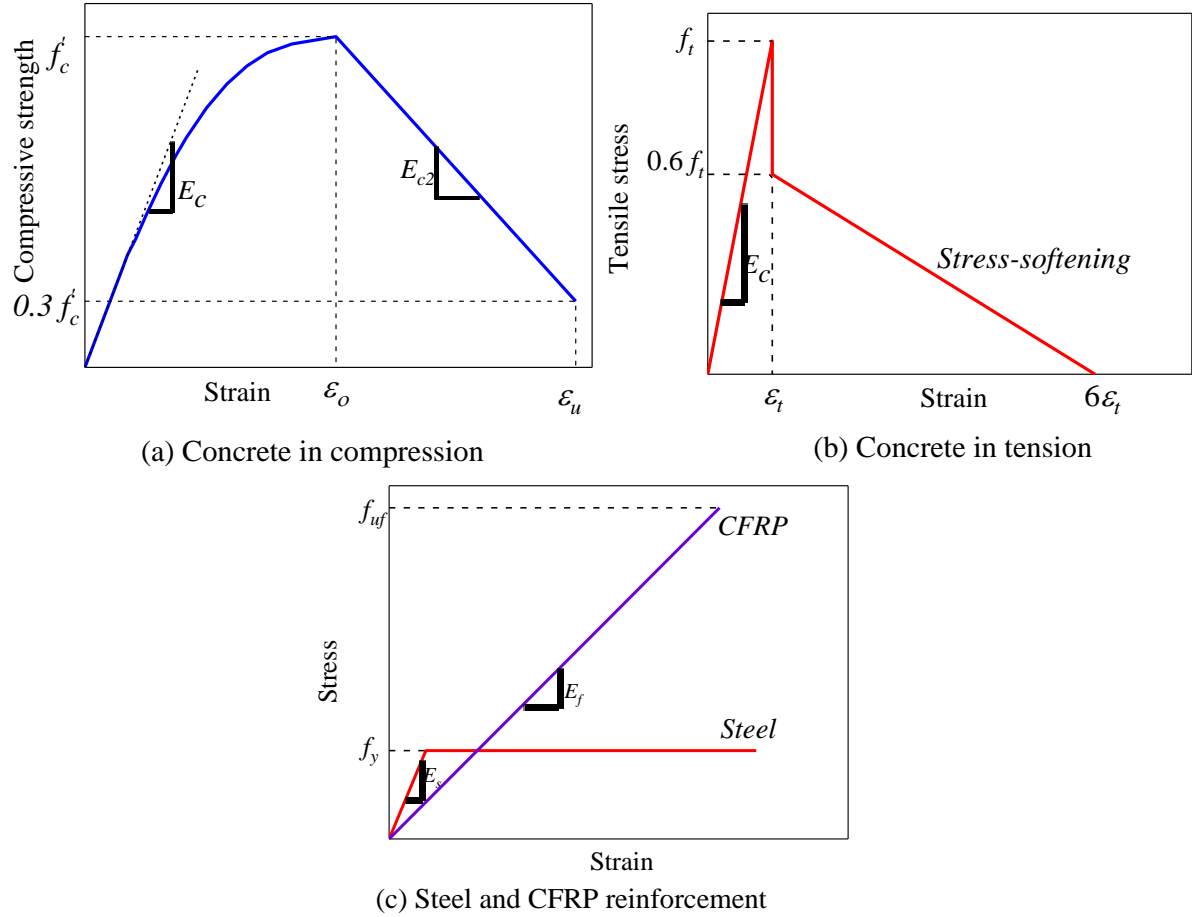


Fig. (3): Constitutive material models.

3.2.5. Contact modelling

The connection between the concrete slab and the CFRP was formed by defining surface-to-surface communication for the ANSYS-software. This contact is a special type of connection. Works the same way as a basic connection type under compact load. The connection algorithm calculations for both normal strength and shear strength in the interface element. Under tensile and shear loads, breaking the separator allows splitting the interconnected surface after a force-based failure criterion.

The bilinear normal stress-gap and shear stress-slip were adopted in the current study as shown in equations below:

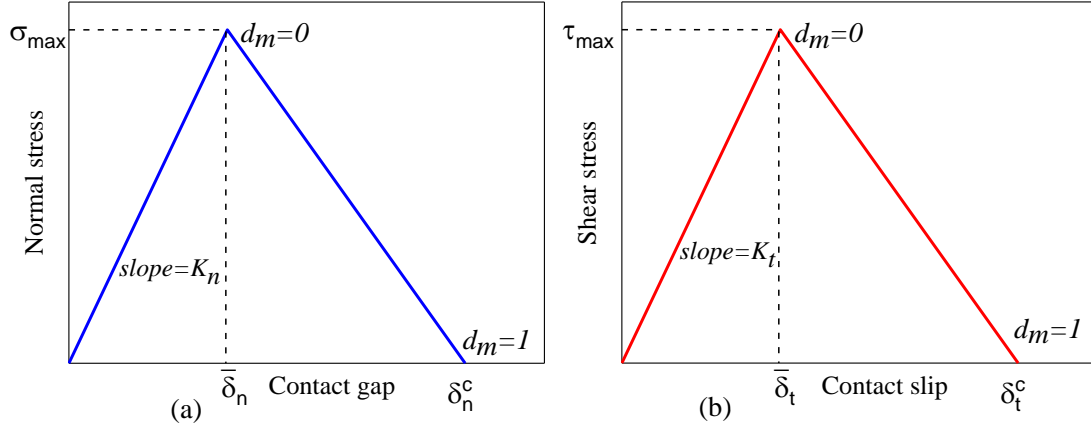
$$\tau_t = K_t \delta_t (1 - d_m) \quad (5)$$

$$\sigma_n = K_n \delta_n (1 - d_m) \quad (6)$$

$$d_m = \left(\frac{\Delta_m - 1}{\Delta_m} \right) \chi \quad (7)$$

$$\Delta_m = \sqrt{\left(\frac{\delta_n}{\delta_n^c}\right)^2 + \left(\frac{\delta_t}{\delta_t^c}\right)^2} \quad (8)$$

$$\chi = \frac{\delta_n^c}{\delta_n^c - \bar{\delta}_n} = \frac{\delta_t^c}{\delta_t^c - \bar{\delta}_t} \quad (9)$$



The shear stress-slip model suggested by [19] was adopted in this study.

$$\tau_{\max} = (0.802 + 0.078\varphi)f_c'^{0.6} \quad (10)$$

$$G_{ct} = \frac{0.976\varphi^{0.526}f_c'^{0.6}}{2} \quad (11)$$

$$\varphi = \frac{\text{Groove depth}+1 \text{ mm}}{\text{Groove width}+2 \text{ mm}} \quad (12)$$

Thus, the calculation of fracture energy of the interface under tensile stress is assumed to be equal to the concrete fracture energy suggested by model code (see equation (15)) [20].

$$\sigma_{\max} = 0.6\sqrt{f_c'} \quad (13)$$

$$G_{cn} = G_{fo} \left(\frac{f_c'}{10}\right)^{0.7} \quad (14)$$

$$G_{ct} = 0.5\tau_{\max}\delta_c^t \quad (15)$$

$$G_{cn} = 0.5\sigma_{\max}\delta_c^n \quad (16)$$

The shear stress-slip and normal stress-gap models were assigned by improving a subroutine in ANSYS order menu to the contact surface.

4. Validation of the FE model

The all FE results are compared with the experimental data to check the accuracy of the FE model, which is including load-deflection curve and ultimate load. Table (3), display comparison between experimental ultimate loads of tested flexural RC slab and the ultimate loads from the numerical analysis by ANSYS program. The variance between the experimental and numerical ultimate loads is not more than (10.96%). Fig. (5) shows the load-deflection obtained from finite element analysis and experimental results. These figures show a good concord between experimental and F.E.A curves.

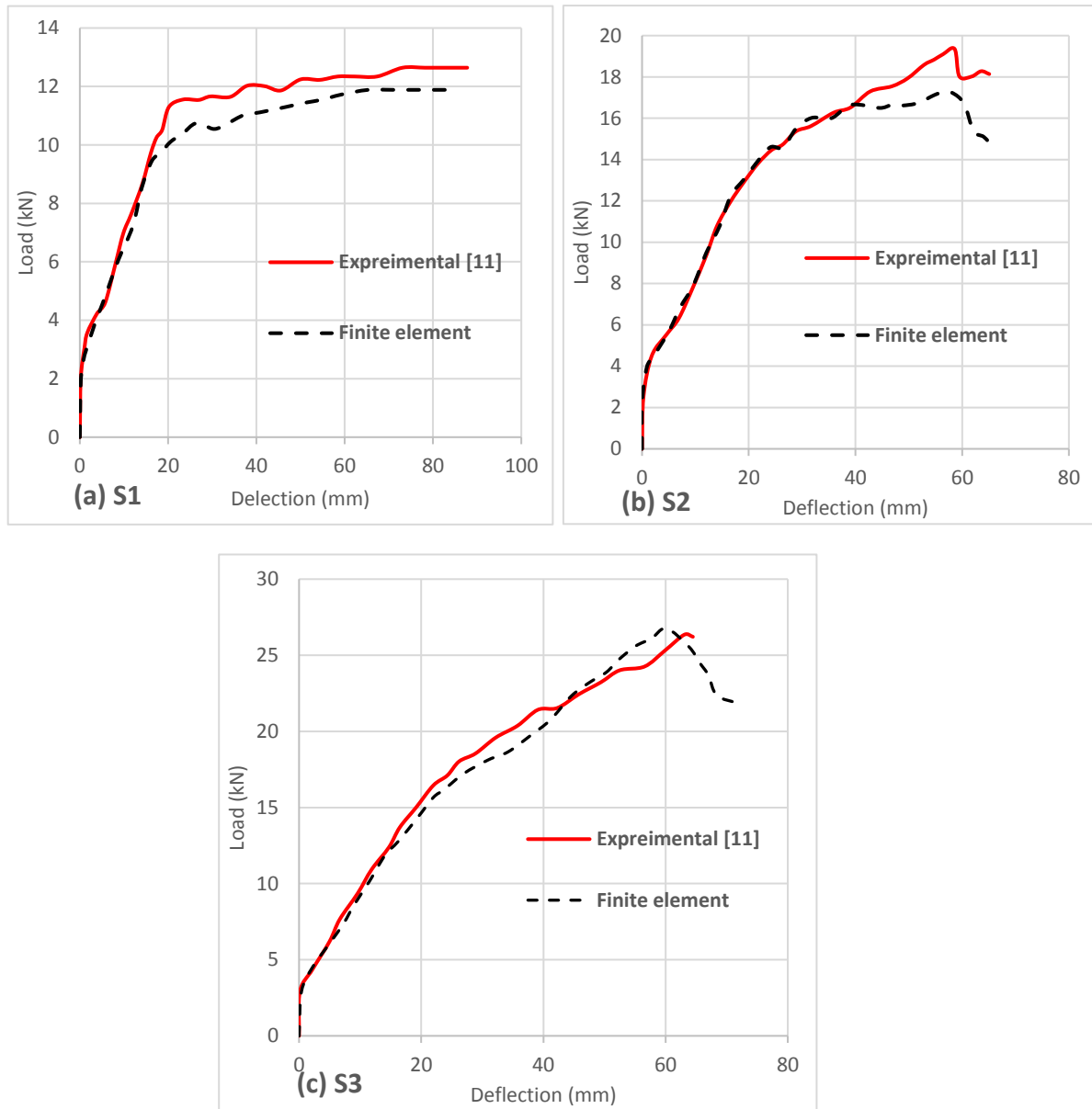


Fig. (5): Comparison of load-deflection curves.

Table (3): Comparison between the FE and experimental results

Specimens	Ultimate load (kN)		
	Experimental	FE	Difference %
S1	12.64	11.88	6.01
S2	19.35	17.23	10.96
S3	26.34	26.76	-1.6

5. Parametric study

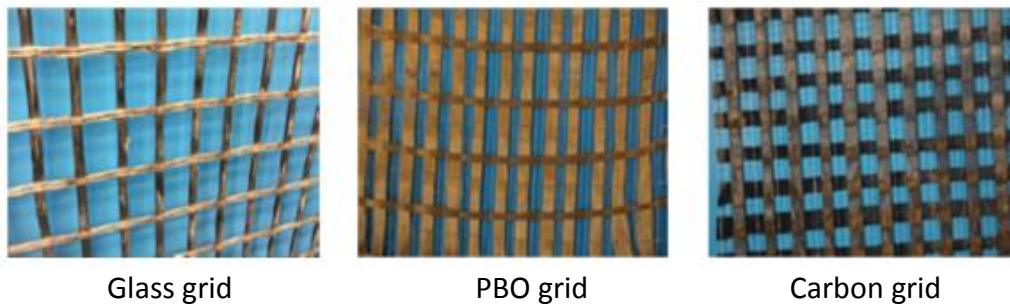
The confirmed FE model was utilized to contemplate the unique parameters on flexural strength of RC slab to archive more information and give more data about the most influential parametric to be considered in design. Table (4) explains these parameters.

Table (4): Variable symbols used in FE study.

Specimens	Type of FCM	Compressive strength (fc) MPa	No. of layers
S4	PBO	41.74	1
S5	Carbon grid	41.74	1
S6	Glass grid	41.74	1
S7	PBO	20	1
S8	PBO	30	1
S9	PBO	50	1
S10	PBO	41.74	2
S11	PBO	41.74	3
S12	PBO	41.74	4

5.1. Effect of FRCM fabric type.

This part discusses the FRCM fabric kind effect on flexural behavior of the RC slab and compared with slab strengthened with CFRP-laminate, these materials were (1) polyparaphenylene benzobisoxazole (PBO), (2) Glass fiber grid and (3) Carbon fiber grid, see Fig.(6). Details of fabric used in FRCM as shown in Table (5). From Fig. (7), it can be seen that the PBO-FRCM had the most critical effect on the extreme load capacity of the strengthened slab. Result specimens (S4), increase (87) % in ultimate strength compared with S1 the control specimens. The deflection at extreme load was in every case minimal than the control slab whereas deflection at failure was nearly the same. The response of the strengthened slabs was evaluated on the load-deflection behaviour. The slab strengthened with FRCM continued to carry loads based on the strengthening composite performance. When the strengthening composite failed, a drop in the load carrying was observed. Then, the trend of load-deflection curves were followed the control slab. In the case that slabs strengthening with CFRP-laminate the continued to carry load to happen the deboning in the interface between composite material and concrete cover.

**Fig. (6): Strengthening composite materials [21].**

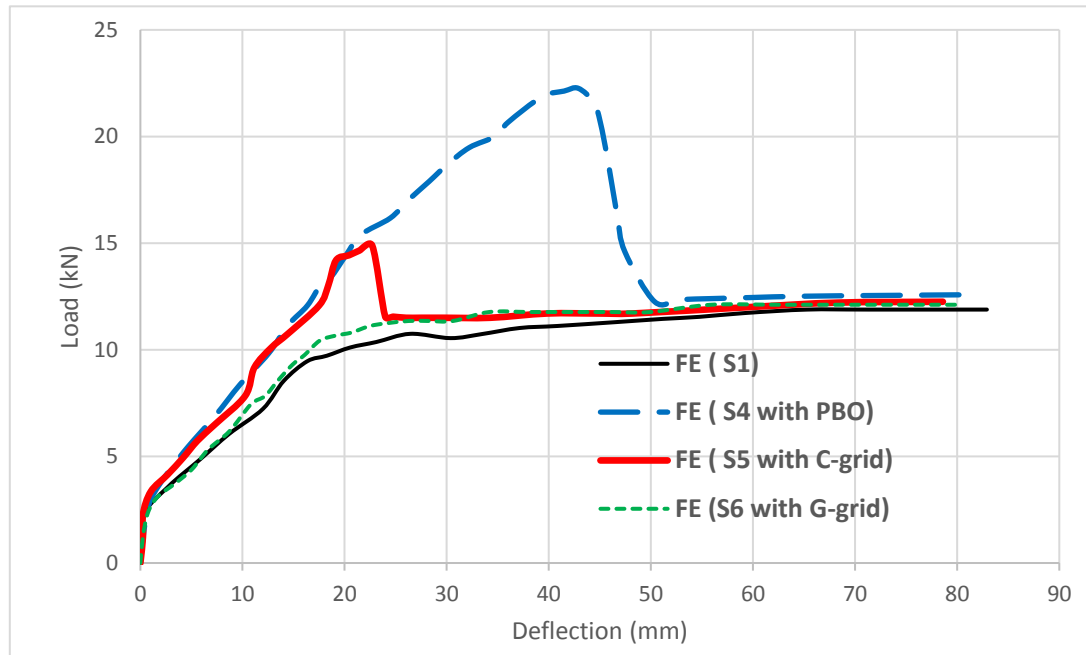


Fig. (7): Simile of load-deflection curves of specimens S1, S4, S5 and S6.

Table (5): Specifics of the fibres utilized in FRCM [21].

Fabric type	Young's modulus (GPa)	Extreme tensile strength MPa	Extreme tensile strain (mm/mm)	Equivalent dry fabric thickness (mm)
Glass	80	2600	1	0.023
PBO	270	5800	1	0.046
carbon	240	4800	1	0.047

5.2. Effect of compressive strength of concrete slab.

The FE model for slab (S4 with PBO) was elected to study the parameter f_c' . The compressive strength f_c' was varied from (20 to 50) MPa to study its impact on the flexural strength. The flexural behaviour was not similar for all models. Strengthened RC slab with minimize compressive strength failed due to concrete strut crushing. On the other hand, it can be concluded that the rise compressive strength of concrete than (30 MPa) decreases the FRCM strengthening impact on the extreme load due to failed occurs in the fibre. Specimens (S9) appear an increase about 7.02 % in extreme load to the specimens (S8). Fig. (8) shows the load-deflection curve for strengthened slab with variables compressive strength.

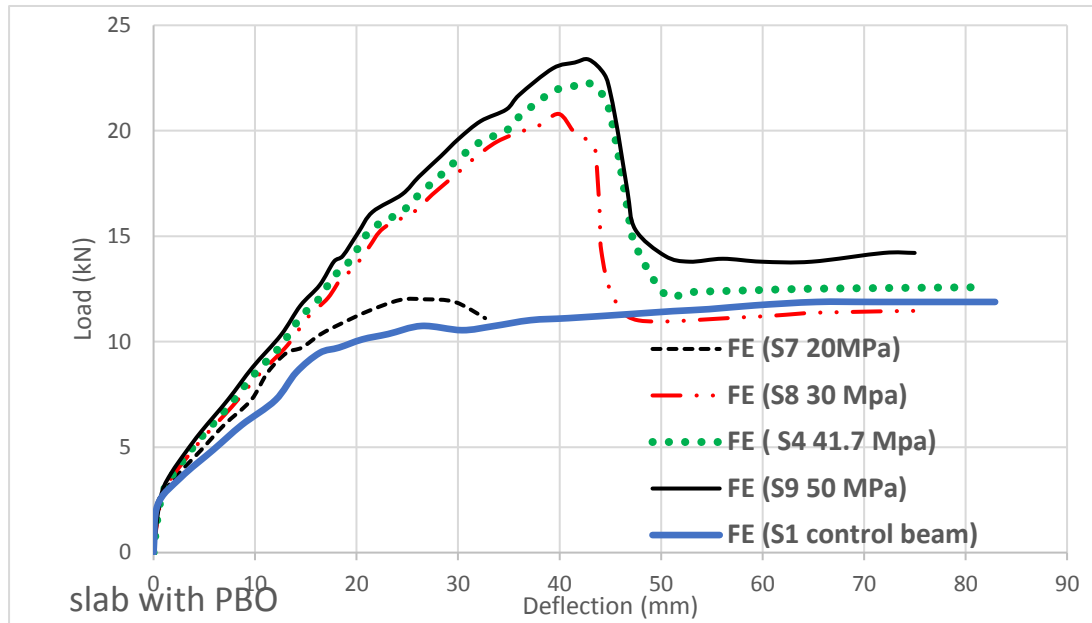


Fig. (8): Comparison of load-deflection curves of specimens S1, S4, S7, S8 and S9.

5.3. Effect of number of fabric layer for FRCM composite.

The number of fabric layers for composite material represented in the FE model to study the effect of this parameter on the flexural performance of strengthened slab. RC slab (S4) selected to study this parameter. Results explained the flexural capacity of the slab with three layers was increasing by (13.84) % compared with same slab with one layer. This performance of flexural behaviour with adding three layers due to increase the axial stiffness of the FRCM. Also, it can be noticed from Fig. (9), that specimens (S12) strengthened by four layers of PBO-FRCM appear increase about (3.86) % compared with S11. Therefore, the increase in the number of layers more than 3 has slightly affected structural behaviour due to failure will occur as a result of concrete crushing.

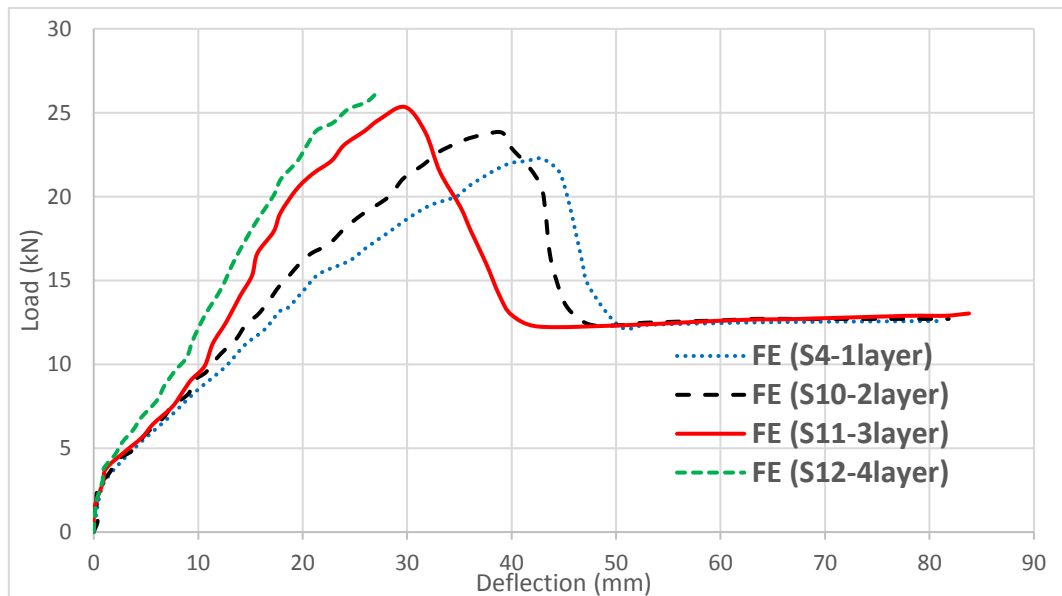


Fig. (9): Simile of load-deflection curves of specimens S4, S10, S11 and S12.

6. Conclusions

According to the previous study, the following conclusions were estimated:

- 1) The three-dimensional nonlinear finite element model displayed in this investigation by utilizing the PC program (ANSYS V.12.1) can reproduce the behavior of reinforced concrete slabs strengthened in flexural with NSM-CFRP. The numerical outcomes were in great concurrence with actual load-deflection curves through the whole scope of behavior.
- 2) The analysis results approved that utilizing of NSM-CFRP system as a strengthening procedure was applicable and can enhance the flexural capability of investigated specimens.
- 3) It was discovered that the variety of FRCM compose really affects the anticipated ultimate load of investigated specimens. Slab strengthened with PBO demonstrated the most noteworthy upgrade in a definitive load limit, as the enhancements were 87%, compared to minimum than 2% for slabs strengthened by glass-FRCM and 25.3% for those strengthened with carbon-FRCM. This was primarily because of the superior bonding that the PBO-FRCM showed with the concrete surface, in which no untimely bonding happened.
- 4) The maximum load increment to (141% and 18.24%) for (S11& S12) respectively with expanding the quantity of texture layers. Be that as it may, the greatest addition as far as the section stack conveying limit is restricted by the compressive quality of cement because of the devastating of cement at pressure zone.
- 5) Results of the parametric investigation demonstrated that values of slabs compressive strength had clear effect on the flexural strength. Then again, a decrease in flexural strength was noticed for lower values of slabs compressive strength. The distinction is because of various failure modes, to be specific fiber break for specimens with higher values of compressive quality and crushing of the concrete strut for bring down values of compressive quality.

Notation:

τ_t and σ_n are the shear and normal contact stresses respectively.

K_t and K_n are the shear and normal contact stiffnesses respectively.

δ_t and δ_n are the relative movement in the tangential and normal directions.

d_m is the debonding parameter.

$\bar{\delta}_n$ and $\bar{\delta}_t$ are the contact gap at the ultimate normal stress and the slip at the ultimate shear stress respectively.

δ_n^c and δ_t^c are the contact gap and slip at the completion of debonding.

τ_{max} is the ultimate contact shear stress.

φ is the aspect ratio of the interface failure plane. f'_c is the compressive strength of concrete. G_{ct} is the shear fracture energy.

σ_{max} is the maximum normal contact stress. G_{cn} is the normal fracture energy.

G_{fo} is the base value of fracture energy depending on the maximum aggregate size.

CONFLICT OF INTERESTS.

- There are no conflicts of interest.

References

- [1] Triantafillou TC, Papanicolaou CG, Zissimopoulos P, Laourdekis T., "Concrete confinement with textile reinforced mortar (TRM) jackets", *ACI Struct* pp.28–37, 2006.
- [2] Triantafillou TC, Papanicolaou CG., "Shear strengthening of reinforced concrete members with textile reinforced mortar (TRM) jackets", *Mater Struct RILEM* pp.93–103, 2006.
- [3] Papanicolaou CG, Triantafillou TC, Bournas DA, Lontou PV., "TRM as strengthening and seismic retrofitting material of concrete structures", In: *Proc of 1st international conference on textile reinforced concrete (ICTRC)*. Germany: RWTH Aachen University; pp. 331–40, 2006.

- [4] Salinas, A.J.O., "Use of grancrete as adhesive for strengthening reinforced concrete structures", Thesis, North Carolina State University, Raleigh, NC, US, 2010.
- [5] Ombres, L., "Flexural analysis of reinforced concrete beams strengthened with cement based high strength composite material", *Composite Structures*, pp. 143-155, 2011.
- [6] Babaeidarabad, S. Loret, G. and Nanni, A. , "Flexural strengthening of RC beams with an externally bonded fabric-reinforced cementitious matrix", *Journal of Composites for Construction*, 10.1061/ (ASCE) CC.1943-5614.0000473, 0401400, 2014.
- [7] Barton, B., Wobbe, E., Dharani, L.R., Silva, P., Birman, V., Nanni A., Alkhrdaji, T., Thomas, J., Tunis, G., "Characterization of reinforced concrete beams strengthened by steel reinforced polymer and grout (SRP and SRG) composites", *Materials Science and Engineering*, A 412, pp.129–136, 2005.
- [8] Pecce, M., Ceroni, F., Prota, A., Gaetano Manfredi, G., "Response prediction of RC beams externally bonded with steel-reinforced polymers", *Journal of Composites for Construction*, DOI: 0.1061/ (ASCE) 1090-0268(2006)10:3(195), 2006.
- [9] ACI (American Concrete Institute), "Guide for the design and construction of externally bonded FRP systems for strengthening concrete structures", ACI 440, Farmington Hills, MI, 2008.
- [10] Napoli, A., and Realfonzo, R. (2015), "Reinforced concrete beams strengthened with SRP/SRG systems: Experimental investigation", *Construction and Building Materials*, pp. 654–677.
- [11] Paulo B., Everaldo B., joaquim A., "Influence of the spacing between NSM-CFRP laminates on the flexural strengthening efficiency of RC slabs", university of patras, pp.11, 2007.
- [12] ANSYS, Release 17.2 Documentation for ANSYS. 2016, Canonsburg, PA, USA
- [13] Kent, D. C, and Park, R., "Flexural members with confined concrete", *Journal of Structures*. Div., ASCE, 97(7), pp.1969-1990, 1971.
- [14] ACI-318-14. *Building Code Requirements for Reinforced Concrete 2014*. American Concrete Institute.
- [15] Kachlakev, D.I., T.H. Miller, T. Potisuk, S.C. YimK. Chansawat, "Finite element modeling of reinforced concrete structures strengthened with FRP laminates", Oregon. Dept. of Transportation. Research Group, 2001.
- [16] Jawdhari A, Harik I, "Evaluation of RC beams strengthened with spliced CFRP rod panels. Proc, Structural Faults and Repair", 2016
- [17] Demakos C. B, Repapis C. C, and Drivas D, "Investigation of structural response of reinforced concrete beams strengthened with anchored FRPs", *Open Construction and Building Technology Journal*, pp.146-57, 2013.
- [18] Piero Colajanni, Fabrizio De Domenico, Antonino Recupero, Nino Spinella , " Concrete columns confined with fibre reinforced cementitious mortars: Experimentation and modelling", *Construction and Building Materials* 52, pp.375-384, 2014.
- [19] Seracino, R., M. Raizal SaifulnazD. Oehlers, "Generic debonding resistance of EB and NSM plate-to-concrete joints", *Journal of Composites for Construction*,. **11**(1): p. 62-70, 2007.
- [20] CEB-FIB, model code 1990. Design Code, 1993.
- [21] Abdulla Jabr, " Flexural Strengthening of RC beams using Fiber Reinforced Cementitious Matrix, FRCM" Degree of Master of Applied Science at the University of Windsor. Pp.135, 2017.

سلوك الانثناء للبلاطات الخرسانية احادية الاتجاه والمقواة بالعجينة الاسمنتية المسلحة بالالياف

علي هادي عظيم

المعهد التقني كربلاء، جامعة الفرات الأوسط التقنية، 56001 كربلاء، العراق.

ali.hadi@kit.edu.iq

عصام محمد علي

المعهد التقني كربلاء، جامعة الفرات الأوسط التقنية، 56001 كربلاء، العراق.

ali_isam@ymail.com

مصطفى صلاح شاكر

المعهد التقني كربلاء، جامعة الفرات الأوسط التقنية، 56001 كربلاء، العراق.

aldulaimy.mustafa93@gmail.com

الخلاصة:

المحاكاة العددية التي أجريت في هذا البحث للتحقيق في سلوك الانحناء للسقوف الخرسانية احادية الاتجاه والمقواة بعجينة اسمنتية مسلحة بالالياف المركبة. تم إجراء تحليل العناصر المحددة ثلاثية الأبعاد باستخدام ANSYS (17.2). تتمثل القضايا الرئيسية التي يركز عليها هذا البحث في: (1) تأثير نوع الالياف المستخدمة في العجينة الاسمنتية على سلوك الانثناء للسقوف الخرسانية من ناحية الحمل الأقصى والهطول، (2) تأثير قيم مختلفة لمقاومة الانضغاط لخرسانة السقف و (3) تأثير عدد طبقات الالياف في العجينة الاسمنتية. بينت النتائج ان نوع الالياف له تأثير واضح على سلوك الانثناء للسقوف المقواة. كما أظهرت الدراسة العديدة أن قوة الانثناء تزداد بزيادة مقاومة انضغاط الخرسانة عندما يكون الفشل محكومًا بسحق الخرسانة. بالإضافة إلى ذلك، كان زيادة عدد طبقات الالياف المركبة تأثير واضح على سلوك السقف الخرساني، ولكن الى عدد محدد لان بعد ذلك يكون الفشل محكوم بتصرف الخرسانة في منطقة الانضغاط.

الكلمات الدالة: المسلحة بالالياف، اتجاه واحد، عجينة الاسمنت المركبة، تقوية.